PHYSICAL REVIEW A VOLUME 54, NUMBER 1 JULY 1996

Electron-impact cross sections involving electronically excited states in H_2 molecules: $B\ ^1\Sigma_u^+ \rightarrow I\ ^1\Pi_g$ transition

R. Celiberto, M. Capitelli, N. Durante,* and U. T. Lamanna
Dipartimento di Chimica Università di Bari and Centro di Studio per la Chimica dei Plasmi del Consiglio Nazionale delle Ricerche, Bari, Italy

(Received 11 December 1995)

Electron-impact cross sections for the process $\mathrm{H}_2(B\ ^1\Sigma_u^+, \nu_i) + e \rightarrow \mathrm{H}_2(I\ ^1\Pi_g) + e$ have been calculated as a function of the collision energy and for different vibrational quantum numbers ν_i in the frame of impact-parameter method. Total and dissociative cross sections are compared with those referred to electronic transitions involving the ground electronic state of H_2 ($X\ ^1\Sigma_g^+ \rightarrow B\ ^1\Sigma_u^+$ and $X\ ^1\Sigma_g^+ \rightarrow C\ ^1\Pi_u$). Moreover, rate coefficients as a function of the vibrational state of the molecule are reported for different temperatures and for both $B \rightarrow I$ and $X \rightarrow B$ transitions, briefly discussing the role of these two processes in the H^- negative-ion production. [S1050-2947(96)04006-1]

PACS number(s): 34.80.Gs, 52.20.Fs

I. INTRODUCTION

A large effort has been devoted in these last years to the calculation of electron-impact cross sections involving H_2 molecules due to their importance in many plasma applications. Basically two lines have been followed in the literature. The first one tries to obtain complete sets of cross sections involving the ground electronic state of H_2 by using the deconvolution of transport coefficients through the Boltzmann analysis, the other one trying to obtain the cross sections by using *ab initio* quantum-mechanical scattering methods. As a result, accurate sets of cross sections do exist which can be confidently used for different plasma situations, in particular, when we do not consider the presence of excited (vibrationally and electronically) states.

The situation completely changes when excited states play an important role in affecting the plasma properties. As an example, it is well known that the production of negative H^- sources strongly depends on the population densities of vibrationally excited states of the ground electronic state ($X\ ^1\Sigma_g^+, \nu_i$), so that the optimization of these sources requires a large effort to understand the dependence of the relevant cross sections on the vibrational quantum number ν_i. This dependence has been recently reviewed by Capitelli *et al.* [1], who have shown that the impact-parameter method is able to give accurate sets of cross sections involving the vibrational manifold of H_2 molecules. Therefore, the knowledge of electron-impact cross sections can be considered satisfactory for transitions involving ground and vibrationally excited molecules.

Unfortunately, an accurate description of H_2 plasmas cannot ignore transitions involving electronically excited states, the cross sections of which are practically unknown. Three examples can be sufficient to emphasize the role of transitions involving electronically excited states in affecting the bulk properties of H_2 plasmas. The first one has been reported by Pinnaduwage and Christophorou [2], who have shown that H^- negative-ion production can be strongly enhanced by laser irradiation of H_2 followed by dissociative attachment of electronically excited states. This means that not only vibrationally excited H_2 molecules, but also electronically excited ones, are responsible for the formation of H^-. Future optimization of negative-ion sources should be based on kinetic models, which also describe the population densities of electronically excited states and therefore should push the researchers to the study of the corresponding cross sections. As a second example, Capitelli and co-workers [3], have recently shown the importance of a second kind of collision [1] involving electronically excited states in affecting the electron energy distribution function (EEDF) of H_2 plasmas.

Last, but not least, the new tokamak machines for ITER (International Thermonuclear Experimental Reactor) are based on the divertor concept, the solution of which requires the knowledge of atomic and molecular processes of edge plasmas which are rich in electronically and vibrationally excited states. All these situations require the development of a collisional radiative model involving both atomic and molecular hydrogen.

In this paper we present a calculation of cross sections involving the electron-impact excitation of the vibrational states of $B\ ^1\Sigma_u^+$ to the vibrational states of $I\ ^1\Pi_g$, i.e., the transition

$$\mathrm{H}_2(B\ ^1\Sigma_u^+, \nu_i = 0-20) + e \rightarrow \mathrm{H}_2(I\ ^1\Pi_g) + e.$$

The impact-parameter method has been considered adequate to obtain a reliable set of cross sections. The results can be used to understand the possible enhancement of cross sections due to the initial electronic excitation of the target. Moreover, a rate coefficient based on a Maxwell electron-energy distribution function has been calculated and compared with the corresponding rates involving the ground electronic state.

In Sec. II we briefly describe the impact-parameter method, while in Sec. III some computational details are

---

*Istituto di Chimica Quantistica ed Energetica Molecolare del Consiglio Nazionale delle Ricerche, Pisa, Italy.

1050-2947/96/54(1)/432(7)/$10.00

given. Results are presented in Sec. IV. Finally, a brief summary is given in Sec. V.

II. METHOD OF CALCULATION

According to the impact-parameter method [4–8] the total cross section for a vibroelectronic excitation at a given collision energy E can be written as

$$\sigma_{\nu_i}^{\alpha_i\rightarrow\alpha_f}(E)=\sum_{\nu_f}\sigma_{\nu_i,\nu_f}^{\alpha_i\rightarrow\alpha_f}(E)+\int d\varepsilon\,\frac{d\sigma_{\nu_i,\varepsilon}^{\alpha_i\rightarrow\alpha_f}(E)}{d\varepsilon},\tag{1}$$

where (ν_i,α_i) and (ν_f,α_f) represent, respectively, the manifold of the vibrational and electronic quantum numbers of the initial and final molecular states. The two terms on the right-hand side of Eq. (1) are the contributions due to the bound-to-bound and bound-to-continuum (dissociative) transitions, respectively. In the last case, ε represents the continuum vibrational energy. Both terms are expressed, according to the impact-parameter method, as a product of a ''structural factor'' $S_{\nu_i,\nu_f}^{\alpha_i,\alpha_f}$ containing all the information about the target, and a ''dynamical factor'' $D_{\nu_i,\nu_f}^{\alpha_i,\alpha_f}$ describing the dynamics of the incident electron.

The cross section for bound-to-bound transition is then written as

$$\sigma_{\nu_i,\nu_f}^{\alpha_i\rightarrow\alpha_f}(E)=S_{\nu_i,\nu_f}^{\alpha_i,\alpha_f}D_{\nu_i,\nu_f}^{\alpha_i,\alpha_f}(E),\tag{2}$$

where the structural factor is given by

$$S_{\nu_i,\nu_f}^{\alpha_i,\alpha_f}=\frac{m^2e^2}{3g_i\hbar^4}\,(2-\delta_{\Lambda_i,0})(2-\delta_{\Lambda_f,0})\times\left|\int_0^\infty dR\,\chi_{\nu_f}^{\alpha_f}(R)M_{\Lambda_i,\Lambda_f}(R)\chi_{\nu_i}^{\alpha_i}(R)\right|^2.\tag{3}$$

In Eq. (3), m, e, $\hbar$, and g_i represent in order the mass and charge of the electron, Planck's constant, and a degeneracy factor for the α_i state. $\chi(R)$ is the vibrational wave function depending on the internuclear distance R, and $M_{\Lambda_i,\Lambda_f}(R)$ is the usual electronic transition dipole moment linking the two electronic states under consideration, characterized by the quantum numbers of the projection of the electronic angular momentum on the internuclear axes Λ_i and Λ_f.

The dynamical factor is expressed as

$$D_{\nu_i,\nu_f}^{\alpha_i,\alpha_f}(E)=\frac{2\pi\hbar^2}{m^2u_i^2}\Bigg[\gamma_i\left(K_0(\gamma_i)K_1(\gamma_i)-\frac{\pi^2}{4}\,S_0(\gamma_i)S_1(\gamma_i)\right)+\gamma_f\left(K_0(\gamma_f)K_1(\gamma_f)-\frac{\pi^2}{4}\,S_0(\gamma_f)S_1(\gamma_f)\right)+\gamma\Bigg(K_0(\gamma_i)K_1(\gamma_f)$$
$$+K_0(\gamma_f)K_1(\gamma_i)+\frac{\pi^2}{4}\,S_0(\gamma_i)S_1(\gamma_f)+\frac{\pi^2}{4}\,S_0(\gamma_f)S_1(\gamma_i)\Bigg)+\left(\frac{u_i^2-u_f^2}{u_i^2+u_f^2}\right)\left(\ln\frac{\gamma_f}{\gamma_i}+\frac{\pi^2}{2}\int_{\gamma_i}^{\gamma_f}S_0(\gamma)d\gamma\right)\Bigg],\tag{4}$$

where K_i and S_i are the modified Bessel functions and modified Struve functions, respectively, and u_i and u_f are the initial and final electron velocities. Moreover,

$$\gamma_i=\frac{\rho_0|\Delta E_{\nu_i,\nu_f}^{\alpha_i,\alpha_f}|}{\hbar}\,\frac{1}{u_i},\tag{5}$$

$$\gamma_f=\frac{\rho_0|\Delta E_{\nu_i,\nu_f}^{\alpha_i,\alpha_f}|}{\hbar}\,\frac{u_i}{u_f^2},\tag{6}$$

$$\gamma=\frac{\rho_0|\Delta E_{\nu_i,\nu_f}^{\alpha_i,\alpha_f}|}{\hbar}\,\frac{2u_i}{u_i^2+u_f^2},\tag{7}$$

where $\Delta E_{\nu_i,\nu_f}^{\alpha_i,\alpha_f}$ is the transition energy defined as

$$\Delta E_{\nu_i,\nu_f}^{\alpha_i,\alpha_f}=\varepsilon_{\nu_f}^{\alpha_f}-\varepsilon_{\nu_i}^{\alpha_i}.\tag{8}$$

ε_ν^α is the νth vibrational eigenvalue belonging to the α electronic state. ρ_0 is a cutoff parameter introduced in the impact-parameter method to avoid divergent cross sections [6,7]. Usually it is determined by requiring that the cross sections calculated in the Born approximation and in the impact parameter method for high energies be the same [6,7]. Details of the calculation are reported in the Appendix.

The cross section for bound-to-continuum transitions keeps the same form of Eq. (2),

$$\int d\varepsilon\,\frac{d\sigma_{\nu_i,\varepsilon}^{\alpha_i\rightarrow\alpha_f}(E)}{d\varepsilon}=\int d\varepsilon\; S_{\nu_i,\varepsilon}^{\alpha_i,\alpha_f}D_{\nu_i,\varepsilon}^{\alpha_i,\alpha_f}(E),\tag{9}$$

where the structural and dynamical factors are given again by Eqs. (3) and (4) by formally replacing the discrete variable ν_f with the continuum energy ε.

III. COMPUTATIONAL DETAILS

The structural factor has been calculated by evaluating the integral appearing in Eq. (3) by using Gauss-Legendre quadrature for bound-to-bound excitation and the trapezoidal rule for the bound-to-continuum case. The vibrational wave functions have been calculated by solving the Schrödinger equation,

$$\left[-\frac{\hbar^2}{2\mu}\,\frac{d^2}{dR^2}+V_\alpha(R)-E_\nu^\alpha\right]\chi_\nu^\alpha(R)=0,\tag{10}$$

TABLE I. Electronic energies as a function of internuclear distance for the $I\ {}^1\Pi_g$ state.

Internuclear distance (a.u.)	Energy (hartree)
0.5	0.210 888 0
0.7	−0.236 982 0

where μ is the reduced mass of the molecule. The wave functions and eigenvalues E_v^α for the bound states have been obtained by expanding $\chi_v^\alpha(R)$ in terms of harmonic oscillators, while for the continuum, $\chi_\varepsilon^\alpha(R)$ has been calculated by using the method reported in Ref. [8]. The $V_\alpha(R)$ electronic potentials for both B and I states have been obtained by linear interpolation of the data of Refs. [9,10]. For short internuclear distances (see Table I), the electronic energies have been obtained by performing full configuration-interaction (CI) calculations (see below). The repulsive branch of the $I\ {}^1\Pi_g$ potential curve has been expressed in the form

$$V_\alpha(R)=A\ \exp(-BR), \tag{11}$$

where the constants A and B have been obtained by performing a simple linear fit at the two smallest internuclear distances reported in Table I [5].

Figure 1 illustrates the potential curves for H_2 for both $B\ {}^1\Sigma_u{}^+$ and $I\ {}^1\Pi_g$ states as well as the $X\ {}^1\Sigma_g^+$ ground state obtained by Kolos and Wolniewicz [11]. The potential curve for the I state [10] shows a double well. The deepest one presents a minimum at $R\approx1.8$ a.u. and supports four vibrational levels ($v_i=0$–3). The second minimum is placed at $R\approx8$ a.u. Although this well is not very deep, it contains five closely spaced vibrational levels. This potential curve also exhibits a maximum above the dissociation energy threshold at $R\approx4.25$ a.u. This barrier determines the presence of a quasibound vibrational state that produces a sharp ''resonance'' in the structural factor around 2×10^{-2} eV above the dissociation limit.

TABLE II. Electronic transition dipole moment as a function of internuclear distance.

Internuclear distance (a.u.)	Dipole moment (a.u.)
0.500	2.127 9
0.700	2.106 0
1.000	2.049 3
1.400	1.892 0
2.000	1.531 9
2.490	1.291 6
3.000	1.084 5
3.001	1.084 1
3.359	0.945 61
3.665	0.802 10
3.946	0.591 57
4.000	0.543 68
4.209	0.364 20
4.461	0.148 80
4.600	0.042 108
4.706	0.032 060
4.800	0.092 609
4.945	0.177 00
5.000	0.206 40
5.181	0.294 00
5.400	0.384 40
5.414	0.389 73
5.646	0.470 10
5.879	0.539 20
6.000	0.571 50
6.111	0.599 15
6.342	0.651 82
7.000	0.775 40
7.774	0.893 80
8.000	0.926 70
9.000	1.087 6
10.00	1.329 4
11.00	1.743 9
12.00	2.277 5

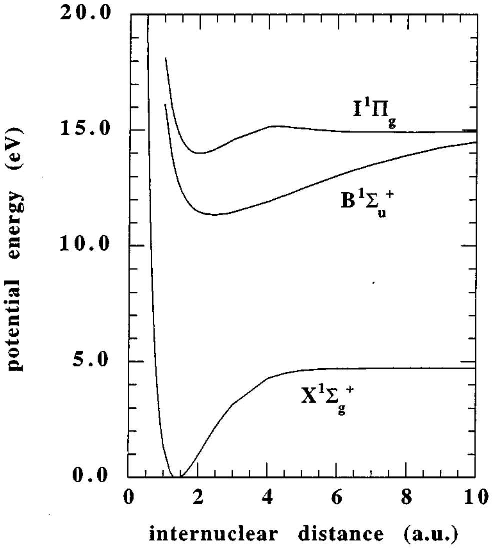

FIG. 1. Potential-energy curves for the $X\ {}^1\Sigma_g^+$, $B\ {}^1\Sigma_u^+$, and $I\ {}^1\Pi_g$ electronic states of H_2 [11,9,10].

The electronic dipole transition moment M_{Λ_i,Λ_f} has been calculated for 34 internuclear distances (see Table II), performing full CI calculations by using three different basis sets of Slater-type orbitals (STO's). Forty-three STO functions were used in the range of $R<2$ a.u., 49 STO functions in the range $2<R<3$ a.u., and 55 STO functions for $R>3$ a.u. The basis included s, p, and d STO's. In the CI calculation all the single and double excitations were considered. The present calculations have been checked by comparing the dipole transition moments for $X\rightarrow B$, $E,F\rightarrow B$, and $X\rightarrow C$ transitions with those obtained by Wolniewicz [12]. A discrepancy not exceeding 3% has been found. The electronic dipole transition moments required in the integration appearing in Eq. (3) were linearly interpolated from the data of Table II.

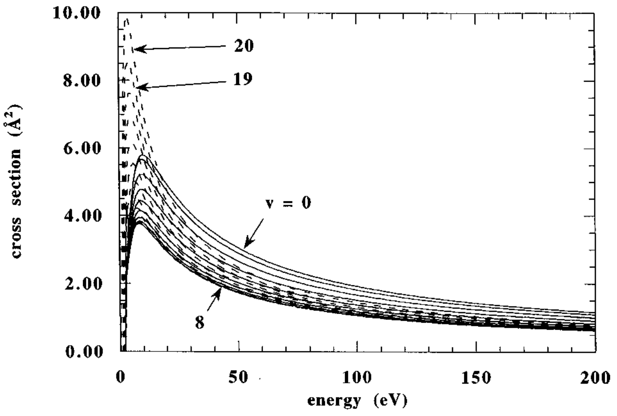

FIG. 2. Total cross sections as a function of collision energy for the process $H_2(B\ ^1\Sigma_u^+, \nu_i = 0-20) + e \rightarrow H_2(I\ ^1\Pi_g) + e$. Solid lines, $\nu_i \leq 8$; dotted lines, $\nu_i > 8$.

IV. RESULTS

Total cross sections for the process,

$$H_2(B\ ^1\Sigma_u^+, \nu_i = 0-20) + e \rightarrow H_2(I\ ^1\Pi_g) + e,$$

involving the first 21 vibrational levels of the $B\ ^1\Sigma_u^+$ state, have been reported in Fig. 2. We can note that the total cross section strongly decreases with initial vibrational quantum number up to $\nu_i = 8$, presenting an opposite trend for $\nu_i > 8$. From $\nu_i = 8$ through $\nu_i = 20$ the cross section increases by a factor of 2, reaching the maximum value of $\sim 10^{-15}$ cm^2 for $\nu_i = 20$ at a collision energy around 5 eV. The behavior of these cross sections can be compared with the corresponding ones for $X \rightarrow B$ and $X \rightarrow C$ electronic transitions [6]. In both cases the cross section initially increases as a function of the vibrational quantum number. For high ν_i values ($\nu_i = 12-14$), the trend is inverted in the case of the $X \rightarrow B$ process, while for the $X \rightarrow C$ transition the cross section becomes independent of ν_i. The behavior of the cross sections with ν_i can be understood in terms of the electronic dipole transition moment [13].

Figure 3 reports the dissociative cross sections as a function of collision energy. The curves in this case show a monotonic enhancement up to $\nu_i = 20$, in contrast with the dissociation in the $X \rightarrow B$ and $X \rightarrow C$ transitions, where the cross sections present an irregular dependence on the vibrational quantum number [8]. The contribution of the dissociation to the total cross section can be better appreciated in Fig. 4. In this figure are reported the total (open circles) and dissociative (closed circles) cross sections as a function of ν_i and for a fixed incident energy of 10 eV. The bound-to-bound contribution can be obtained by difference. Inspection of this figure shows that the dissociative cross section is negligible for very low ν_i values ($\nu_i = 0,1$), becoming the main contribution to the total cross section for $\nu_i > 10$. Once again a different situation is found in the above transitions involving the X ground state. For instance, the dissociative cross sections for $X \rightarrow B$ and $X \rightarrow C$ excitations in hydrogen and deuterium, have been found [6] to be about one or more orders of magnitude smaller than the corresponding bound-bound cross sections, in all the investigated ν_i range. Actually, the low contribution of bound-to-bound cross sections for the $B \rightarrow I$ transition is mainly determined by the overlap between the vibrational wave functions in the structural factor. This observation is confirmed by the behavior of the Franck-Condon factors calculated by Spindler [14] for this transition. The sum on ν_f of the Franck-Condon factors converges to unity only for the first few vibrational levels of B state, while for high ν_i the departure from unity becomes very large, giving a measure of the dissociative transition contribution.

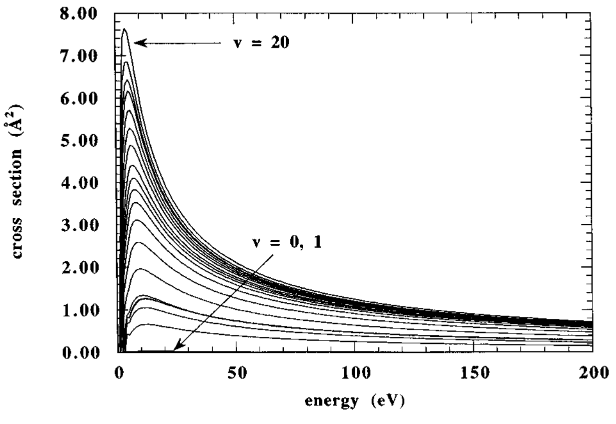

FIG. 3. Dissociative cross sections as a function of collision energy for the process $H_2(B\ ^1\Sigma_u^+, \nu_i = 0-20) + e \rightarrow H_2(I\ ^1\Pi_g) + e$.

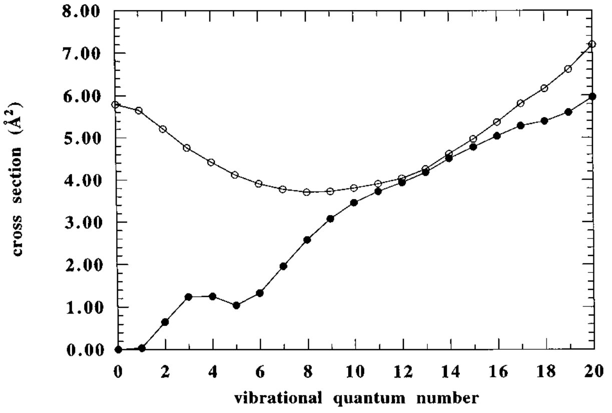

FIG. 4. Cross sections as a function of initial vibrational quantum number for the process $H_2(B\ ^1\Sigma_u^+, \nu_i = 0-20) + e \rightarrow H_2(I\ ^1\Pi_g) + e$ at a fixed collision energy $E = 10$ eV. Open circles, total cross sections [Eq. (1)]; closed circles, dissociative cross sections [Eq. (9)].

V. CONCLUSION

In the present paper we have presented a quantum-mechanical calculation of electron-impact cross sections involving electronically excited states. The present data represent, to our knowledge, one of the few examples of this kind of cross section. As a general comment, we can say that the present calculations confirm some expected trends, such as the decrease of the threshold energy, as well as the increase of the magnitude of the cross section as compared with the corresponding values for molecules in the ground electronic state.

A deeper insight of the results shows the peculiarities of

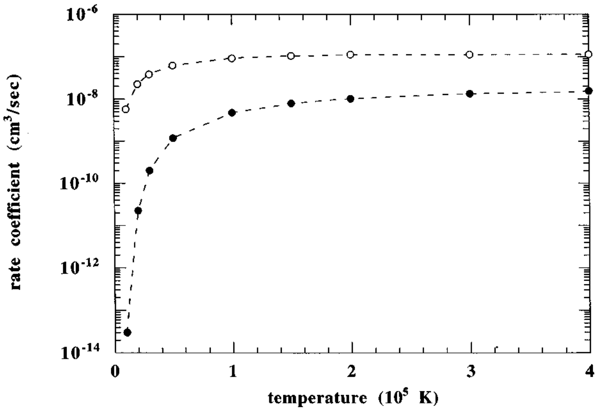

FIG. 5. Rate coefficients as a function of the electron temperature for the processes

$$H_2(B\ ^1\Sigma_u^+, \nu_i=0)+e \rightarrow H_2(I\ ^1\Pi_g)+e \quad \text{(open circles)},$$
$$H_2(X\ ^1\Sigma_g^+, \nu_i=0)+e \rightarrow H_2(B\ ^1\Sigma_u^+)+e \quad \text{(closed circles)}.$$

the present calculations. In particular, we observe a monotonic increase of the cross section as a function of initial vibrational quantum number, as well as the predominance of dissociative channels (bound-free transitions) compared to bound-bound ones.

Coming back to the comparison of this kind of cross section with the corresponding ones starting from the ground state, we can say that the differences both in the energy threshold and in the maximum of the cross section will propagate to a larger extent into rate coefficients, i.e., in the quantity

$$K_\nu^{\alpha_i \rightarrow \alpha_f} = \left(\frac{2}{\mu}\right)^{1/2} \int dE\ \sigma_\nu^{\alpha_i \rightarrow \alpha_f}(E)\sqrt{E} f(E), \tag{12}$$

where $f(E)$ is the Maxwellian distribution function for free electrons. Figure 5 compares the rate coefficients as a function of electron temperature for $X \rightarrow B$ and $B \rightarrow I$ transitions, while Fig. 6 reports the same quantities as a function of vibrational quantum number at a given electron temperature.

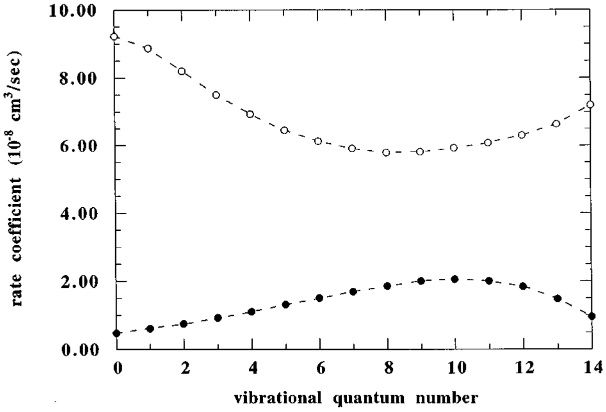

FIG. 6. Rate coefficients as a function of the vibrational quantum number and for a fixed electron temperature $T=10^5$ K for the processes

$$H_2(B\ ^1\Sigma_u^+, \nu_i=0)+e \rightarrow H_2(I\ ^1\Pi_g)+e \quad \text{(open circles)},$$
$$H_2(X\ ^1\Sigma_g^+, \nu_i=0)+e \rightarrow H_2(B\ ^1\Sigma_u^+)+e \quad \text{(closed circles)}.$$

At low electron temperature, threshold effects dominate the rates so that the coefficients for the $B \rightarrow I$ transition are several orders of magnitude larger than the $X \rightarrow B$ transition. At high electron temperatures, threshold effects decrease their importance so that the difference in the rates for the two transitions mainly depends on differences in the corresponding maximum. The relevant rates, as a function of the vibrational quantum number, at high temperature, follow the maximum of the cross sections, as can be understood from Fig. 6.

As a final comment, we want to discuss how the present rates can affect the production of negative ions [15]. According to the adopted kinetic scheme, negative ions H^- are produced by dissociative attachment from vibrational states of the ground electronic state of H_2. These states are in turn formed by electron-impact excitation of B and C states followed by radiative decay on the X state. In this scheme it is implicit that radiative decay from the B state is the only mechanism depopulating this state. On the other hand, collisional excitation to the I state can be taken as indicative of the importance of electron-impact processes in depopulating the B state. Insertion of this channel (or of similar ones) in the whole kinetics, should be important when the collisional rate $n_e K_\nu^{B \rightarrow I}$ (sec^{-1}) is of the same order of magnitude of transition probabilities linking the B and X states. Keeping in mind that these latter are of the order of 10^7–10^9 sec^{-1} we can understand that electron densities of the order of 10^{14}–10^{16} cm^{-3} are necessary to compete with radiative decay. At lower electron density these transitions should also be important to transport part of the energy transferred to the B state to the high-lying excited states, in particular to Rydberg states, which can also be important in the production of negative ions.

TABLE III. Cutoff parameter ρ_0 as a function of the vibrational quantum number ν_i.

ν_i	ρ_0 (a.u.)
0	4.60
1	4.46
2	4.50
3	4.56
4	4.55
5	4.55
6	4.52
7	4.48
8	4.45
9	4.38
10	4.30
11	4.25
12	4.20
13	4.10
14	3.90
15	3.75
16	3.60
17	3.48
18	3.50
19	3.55
20	3.60

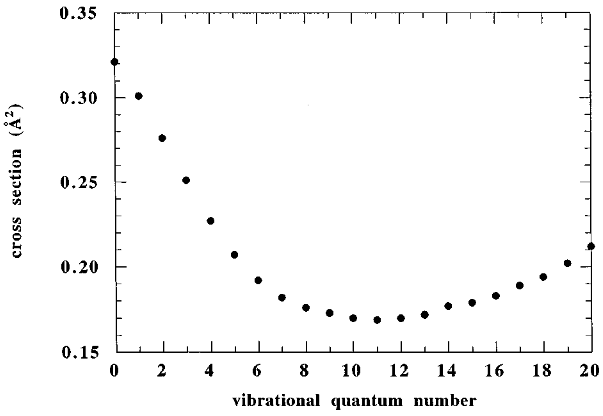

FIG. 7. Born approximation cross sections as a function of the vibrational quantum number, calculated for a fixed energy of 1000 eV, for the process $H_2(B\,^1\Sigma_u^+, \nu_i=0-20)+e\rightarrow H_2(I\,^1\Pi_g)+e$.

ACKNOWLEDGMENTS

This work has been partially supported by Ministero Università e Ricerca Scientifica e Tecnologica, as well as by Network EBRCHRXCT920003 ''negative-ion production by volume and surface processes in plasmas.''

APPENDIX

The cutoff parameter ρ_0 appearing in the definition of the dynamical factor, Eq. (4), can be obtained by comparing the impact-parameter cross section and the Born approximation for very high energies. The total rotational averaged differential cross section in the Born approximation is given by [16]

$$\left(\frac{d\sigma}{d\Omega}\right)_{\text{total}}=\sum_{\nu_f}\frac{k_f}{k_i}\int\frac{d\hat{\mathbf{R}}}{4\pi}\left|\int dR\langle\nu_f|\varepsilon(R,\hat{\mathbf{R}},K)|\nu_i\rangle\right|^2, \tag{A1}$$

where

$$\varepsilon(R,\hat{\mathbf{R}},K)=\frac{2e^2m}{(\hbar K)^2}\langle\Psi_{\alpha_f}|\sum_j e^{i\mathbf{K}\cdot\mathbf{r}_j}|\Psi_{\alpha_i}\rangle.$$

Ψ_α is the electronic wave function for the α state, depending on the electron coordinates $\mathbf{r}_j$ and parametrically on the internuclear distance R, and $\mathbf{K}=\mathbf{k}_i-\mathbf{k}_f$. $\hat{\mathbf{R}}$ is the versor defining the orientation of the molecule in the laboratory frame. The sum is extended also to the continuum states. Assuming k_f is independent of the final vibrational quantum number ν_f [17], Eq. (A1) can be written as

$$\left(\frac{d\sigma}{d\Omega}\right)_{\text{total}}\approx\frac{\overline{k}}{k_i}\sum_{\nu_f}\int\frac{d\hat{\mathbf{R}}}{4\pi}\left|\int dR\langle\nu_f|\varepsilon(R,\hat{\mathbf{R}},K)|\nu_i\rangle\right|^2, \tag{A2}$$

where $\overline{k}$ is set to a particular value of k_f. Using the closure relation $\Sigma_{\nu_f}|\nu_f\rangle\langle\nu_f|=1$, we find

$$\left(\frac{d\sigma}{d\Omega}\right)_{\text{total}}\approx\frac{\overline{k}}{k_i}\left\langle\nu_i\left|\int\frac{d\hat{\mathbf{R}}}{4\pi}|\varepsilon(R,\hat{\mathbf{R}},K)|^2\right|\nu_i\right\rangle. \tag{A3}$$

Defining now the generalized oscillator strength $f(K)$ as [16],

$$f(K)=\frac{(\hbar K)^2\Delta E_{\alpha_i\alpha_f}(R)}{2me^4}\int\frac{d\hat{\mathbf{R}}}{4\pi}|\varepsilon(R,\hat{\mathbf{R}},K)|^2, \tag{A4}$$

we get for the integral cross section $\sigma^B_{\text{total}}(E)$ in the Born approximation:

$$\sigma^B_{\text{total}}(E)=\int d\Omega\left(\frac{d\sigma}{d\Omega}\right)_{\text{total}}$$

$$=\left\langle\nu_i\left|\left[\frac{4\pi me^4}{(\hbar k_i)^2\Delta E_{\alpha_i\alpha_f}(R)}\int_{|k_i-k_f|}^{k_i+k_f}dK\,\frac{1}{K}\,f(K)\right]\right|\nu_i\right\rangle.$$

Finally, Eq. (A5) can be written in the simple form

$$\sigma^B_{\text{total}}(E)=\langle\nu_i|\sigma^B_{\alpha_i\rightarrow\alpha_f}(E;R)|\nu_i\rangle, \tag{A6}$$

where $\sigma^B_{\alpha_i\rightarrow\alpha_f}(E;R)$, the expression in the square brackets of Eq. (A5), is the $\alpha_i\rightarrow\alpha_f$ vertical-transition cross section parametrically depending on the internuclear distance R.

Adjusting properly the cutoff parameter ρ_0 in Eq. (1), we imposed the condition that the impact parameter [Eq. (1)] and the Born approximation cross section [Eq. (A6)] calculated at $E=1000$ eV be the same.

The obtained cutoff parameters are reported in Table III, while the Born cross sections calculated from Eq. (A6) at 1000 eV as a function of the vibrational quantum number are shown in Fig. 7.

---

[1] M. Capitelli, R. Celiberto, and M. Cacciatore, in *Advances in Atomic Molecular, and Optical Physics, Cross Section Data*, edited by M. Inokuti (Academic, New York, 1994), Vol. 33, p. 321.

[2] L. A. Pinnaduwage and L. G. Christophorou, Phys. Rev. Lett. **70**, 754 (1993).

[3] G. Colonna, C. Gorse, M. Capitelli, R. Winkler, and J. Wilhelm, Chem. Phys. Lett. **213**, 5 (1993).

[4] A. H. Hazi, Phys. Rev. A **23**, 2232 (1981).

[5] M. J. Redmon, B. C. Garrett, L. T. Redmon, and C. W. McCurdy, Phys. Rev. A **32**, 3354 (1985).

[6] R. Celiberto and T. N. Rescigno, Phys. Rev. A **47**, 1939 (1993).

[7] B. C. Garrett, L. T. Redmon, C. W. McCurdy, and M. J. Redmon, Phys. Rev. A **32**, 3366 (1985).

[8] R. Celiberto, U. T. Lamanna, and M. Capitelli, Phys. Rev. A **50**, 4778 (1994).

[9] L. Wolniewicz and K. Dressler, J. Chem. Phys. **88**, 3861 (1988).

[10] W. Kolos and J. Rychlewski, J. Mol. Spectrosc. **66**, 428 (1977).

[11] W. Kolos and L. Wolniewicz, J. Chem. Phys. **43**, 2429 (1965).

[12] L. Wolniewicz, J. Chem. Phys. **51**, 5002 (1969).

[13] R. Celiberto, M. Capitelli, and R. K. Janev, Chem. Phys. Lett. (to be published).

[14] R. J. Spindler, J. Quant. Spectrosc. Radiat. Transfer **9**, 597 (1969).

[15] C. Gorse, R. Celiberto, M. Cacciatore, A. Lagana’, and M. Capitelli, Chem. Phys. **161**, 211 (1992).

[16] M. Inokuti, Rev. Mod. Phys. **43**, 297 (1971).

[17] G. P. Arrighini, F. Biondi, and C. Guidotti, Mol. Phys. **41**, 1501 (1980).